Date of issue: June 2006

JUNCAP2

level 200.1

A.J. Scholten, M. Durand, G.D.J. Smit, and D.B.M. Klaassen

Authors' address data: A.J. Scholten; andries.scholten@philips.com
M. Durand;
G.D.J. Smit; gert-jan.smit@philips.com
D.B.M. Klaassen; d.b.m.klaassen@philips.com

Contents

History of model and documentation

Introduction

The first version of the compact MOS model JUNCAP2, Level 200, has been released to the public domain in April 2005. Changes and additions to the model are documented by adapting or extending the documentation in this Report.

History of the model

April 2005 Release of JUNCAP2, level 200 as part of SiMKit 2.1. A Verilog-A implementation is made available as well.

August 2005 Release of JUNCAP2, level 200.1 as part of SiMKit 2.2. Similar to the previous version, a Verilog-A implementation of the JUNCAP2-model is made available as well. Focus of this release was mainly on the optimization of the evaluation speed of JUNCAP2. This new version is fully parameter compatible with the previous version.

The following changes have been made:

- limiting of charge model and of $w_{\mathrm{SRH,step}}$ is now based on the minimum of three built-in voltages, instead of separate limiting for bottom, STI-edge, and gate-edge component;
- limiting of V_{j} to $V_{\mathrm{j,SRH}}$ in Shockley-Read-Hall model replaced by adopting $\mathrm{VMAX/IMAX}$-construction of ideal-current model; subsequently the original $V_{\mathrm{j,SRH2}}$ has been renamed into $V_{\mathrm{j,SRH}}$;
- limiting of V_{AK} to V_{j} in charge model changed from ln-exp type into so-called hyp5 function; limiting of V_{AK} to $V_{\mathrm{j,SRH}}$ (i.e. the previous $V_{\mathrm{j,SRH2}}$) in Shockley-Read-Hall model changed from ln-exp type into so-called hyp2 function.
- expression for Δw_{SRH} rewritten im more concise form (mathematically identical to previous version), see Eq. (4.12).

History of the documentation

April 2005 First release of JUNCAP2, level 200 documentation.

August 2005 Documentation updated for JUNCAP2, level 200.1 release. Section 4.3 has been added to document the so-called hyp-functions introduced in level 200.1.

March 2006 Documentation update. Section 6.7 has been added.

June 2006 Documentation update. Error in Eq. (4.20), which defines b_{TAT}, is corrected.

1 Introduction

The JUNCAP2 model is intended to describe the behavior of the diodes that are formed by the source, drain, or well-to-bulk junctions in MOSFETs. It is the successor of the JUNCAP level=1 model [1].

Whereas the JUNCAP level=1 model gives a satisfactory description of the junction capacitances, its description of diode leakage currents is rather poor for present-day CMOS technologies. This is due to ever increasing doping concentrations in the junctions, leading to increasing electric fields. Due to these high electric fields, leakage mechanisms such as trap-assisted tunneling and band-to-band tunneling have gained importance to such an extent, that they are starting to contribute to the MOSFET off-state current. Thus, accurate modelling of these leakage currents is called for.

In addition to its relevance for advanced CMOS technologies, accurate junction modelling is also relevant for partially depleted SOI (PDSOI). Here, a small positive voltage at the floating body exists, which is determined by the equilibrium between impact ionization and gate current on one hand and current through the source junction on the other hand. Due to the back-gate effect, this small positive floating body voltage gives rise to additional drain current, where it is visible as the so-called "kink effect". Thus, for PDSOI applications, accurate junction modelling in the low-forward regime is required.

2 Summary of physics behind JUNCAP2

The JUNCAP2 model has been developed for the description of source and drain junctions in MOSFETs. The model equations have been developed for symmetrical junctions of arbitrary grading coefficient. The following physical effects have been included:

Geometrical scaling

JUNCAP2 models the capacitances and currents of bottom-, STI-edge, and gate-edge components. This is illustrated in Figs. 2.1 and 2.2.

Depletion capacitance

The depletion capacitance model, similar to JUNCAP level=1, is a standard textbook equation. It has been safeguarded against numerical overflow in the forward mode of operation.

Ideal current

The ideal diode current is modelled using the ideal-case Shockley equation. The bandgap has been made a free parameter to be able to tune the temperature dependence. No (unphysical) ideality factor has been included. Non-idealities are modelled with physics-based equations, as outlined below.

Shockley-Read-Hall current

The Shockley-Read-Hall current is calculated by integrating the Shockley-Read-Hall generation-recombination rate over the depletion region. This is done for arbitrary grading coefficient and results in a single-piece expression in forward and reverse mode of operation.

Trap-assisted tunneling current

The trap-assisted tunneling current is calculated in a similar fashion as the Shockley-Read-Hall current. Now also the field-enhancement factor [2] is taken into account in the calculation. In contrast to e.g. Diode Level 500 [1], the calculation is not based on the low-field approximation of this field-enhancement factor, but is generally valid for both low and high fields. The calculation results in a single-piece expression which is valid in both the forward and reverse regime, and for arbitrary grading coefficient.

Band-to-band tunneling current

For the band-to-band tunneling current, a physical model similar to the Diode Level 500 [1] equation has been implemented. Some additional freedom in fitting the (small) temperature dependence of this current is provided.

Avalanche breakdown

For avalanche breakdown, an expression has been derived which is a simplified form of the Diode Level 500 [1] equations for this phenomenon. In comparison with Diode Level 500, some additional freedom in fitting the onset to breakdown is provided.

Noise

In partially depleted silicon-on-insulator (PD SOI), the shot noise of the junction current is important because, together with the shot noise of the impact ionization current of the MOSFET, it leads to additional Lorentzian noise in the drain current [3]. Therefore, shot noise has been implemented in JUNCAP2.

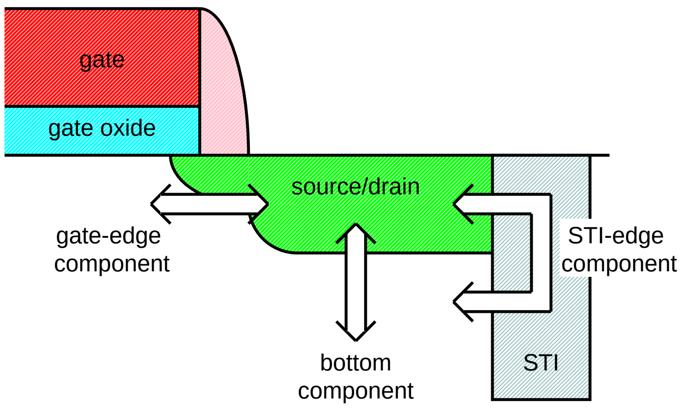

Figure 2.1: The three contributions to the source/drain junction of a MOSFET

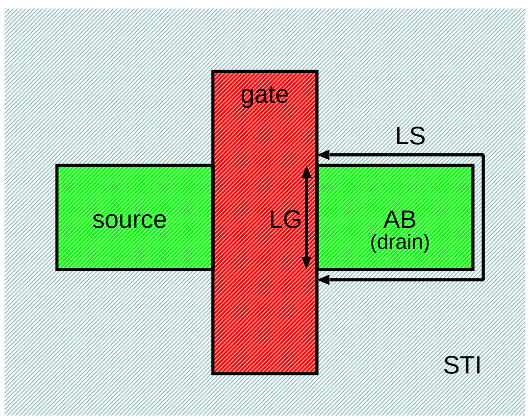

Figure 2.2: Schematic top view of the MOSFET. The meaning of the instance parameters **AB**, **LS**, and **LG** is indicated in the drain region.

3 Model parameters and constants

3.1 Physical Constants

No.	Symbol	Unit	Value	Description
1	T_0	K	273.15	offset between Celsius and Kelvin temperature scale
2	k_{B}	J/K	$1.3806505 \cdot 10^{-23}$	Boltzmann constant
3	q	C	$1.6021918 \cdot 10^{-19}$	elementary charge
4	$\hbar$	Js	$1.05457168 \cdot 10^{-34}$	reduced Planck constant
5	m_0	kg	$9.1093826 \cdot 10^{-31}$	electron rest mass
6	ϵ_{Si}	F/m	$1.045 \cdot 10^{-10}$	absolute permittivity of silicon

3.2 Other constants

No.	Symbol	Unit	Value	Description
1	T_{min}	^{0}C	-250	minimum temperature for model equations
2	$V_{\mathrm{bi,low}}$	V	0.050	lower boundary for built-in voltage
3	a	-	2	sets upper limit of forward capacitance to $a \cdot C_{\mathrm{jo}}$
4	ϵ_{ch}	-	0.1	smoothing constant for charge model
5	ϵ_{av}	-	1×10^{-6}	smoothing constant for effective voltage in avalanche model
6	$V_{\mathrm{br,max}}$	V	1×10^{3}	upper limit for $\mathbf{VBR}$; for larger values, avalanche model is switched off
7	α_{av}	-	0.999	below $-\alpha_{\mathrm{av}} \cdot \mathbf{VBR}$ avalanche model is linearized
8	$V_{\mathrm{max,large}}$	V	1×10^{8}	value assigned to V_{max} when I_{DSAT} is zero.
9	a_{erfc}	-	0.29214664	parameter in erfc approximation
10	p_{erfc}	-	$\sqrt{\pi} \cdot a_{\mathrm{erfc}}$	parameter in erfc approximation
11	b_{erfc}	-	$\dfrac{6 - 5 \cdot a_{\mathrm{erfc}} - p_{\mathrm{erfc}}{}^{-2}}{3}$	parameter in erfc approximation
12	c_{erfc}	-	$1 - a_{\mathrm{erfc}} - b_{\mathrm{erfc}}$	parameter in erfc approximation

3.3 Instance parameters

No.	Name	Unit	Default	Min.	Max.	Description
1	**AB**	m^2	1×10^{-12}	0	–	junction area
2	**LS**	m	1×10^{-6}	0	–	STI-edge part of junction perimeter
3	**LG**	m	1×10^{-6}	0	–	gate-edge part of junction perimeter
4	**MULT**	-	1	0	–	multiplication factor

3.4 Model parameters

No.	Name	Unit	Default	Min.	Max.	Description
0	**LEVEL**	-	200	200	200	level must be 200
1	**TYPE**	-	1	–	–	switch (-1 or 1) to select $p-n$ and $n-p$ junction
2	**TRJ**	$^{\mathrm{o}}$C	21	T_{min}	–	reference temperature
3	**DTA**	$^{\mathrm{o}}$C	0	–	–	temperature offset with respect to ambient temperature
4	**IMAX**	A	1000	1×10^{-12}	–	maximum current up to which forward current behaves exponentially
Capacitance parameters						
5	**CJORBOT**	F/m^2	1×10^{-3}	1×10^{-12}	–	zero-bias capacitance per unit-of-area of bottom component
6	**CJORSTI**	F/m	1×10^{-9}	1×10^{-18}	–	zero-bias capacitance per unit-of-length of STI-edge component
7	**CJORGAT**	F/m	1×10^{-9}	1×10^{-18}	–	zero-bias capacitance per unit-of-length of gate-edge component
8	**VBIRBOT**	V	1	$V_{\mathrm{bi,low}}$	–	built-in voltage at the reference temperature of bottom component
9	**VBIRSTI**	V	1	$V_{\mathrm{bi,low}}$	–	built-in voltage at the reference temperature of STI-edge component
10	**VBIRGAT**	V	1	$V_{\mathrm{bi,low}}$	–	built-in voltage at the reference temperature of gate-edge component
11	**PBOT**	-	0.5	0.05	0.95	grading coefficient of bottom component
12	**PSTI**	-	0.5	0.05	0.95	grading coefficient of STI-edge component
13	**PGAT**	-	0.5	0.05	0.95	grading coefficient of gate-edge component
Ideal-current parameters						
14	**PHIGBOT**	V	1.16	–	–	zero-temperature bandgap voltage of bottom component
15	**PHIGSTI**	V	1.16	–	–	zero-temperature bandgap voltage of STI-edge component
16	**PHIGGAT**	V	1.16	–	–	zero-temperature bandgap voltage of gate-edge component

No.	Name	Unit	Default	Min.	Max.	Description
17	**IDSATRBOT**	A/m^2	1×10^{-12}	0	–	saturation current density at the reference temperature of bottom component
18	**IDSATRSTI**	A/m	1×10^{-18}	0	–	saturation current density at the reference temperature of STI-edge component
19	**IDSATRGAT**	A/m	1×10^{-18}	0	–	saturation current density at the reference temperature of gate-edge component
Shockley-Read-Hall parameters						
20	**CSRHBOT**	A/m^3	1×10^{2}	0	–	Shockley-Read-Hall prefactor of bottom component
21	**CSRHSTI**	A/m^2	1×10^{-4}	0	–	Shockley-Read-Hall prefactor of STI-edge component
22	**CSRHGAT**	A/m^2	1×10^{-4}	0	–	Shockley-Read-Hall prefactor of gate-edge component
23	**XJUNSTI**	m	1×10^{-7}	1×10^{-9}	–	junction depth of STI-edge component
24	**XJUNGAT**	m	1×10^{-7}	1×10^{-9}	–	junction depth of gate-edge component
Trap-assisted tunneling parameters						
25	**CTATBOT**	A/m^3	1×10^{2}	0	–	trap-assisted tunneling prefactor of bottom component
26	**CTATSTI**	A/m^2	1×10^{-4}	0	–	trap-assisted tunneling prefactor of STI-edge component
27	**CTATGAT**	A/m^2	1×10^{-4}	0	–	trap-assisted tunneling prefactor of gate-edge component
28	**MEFFTATBOT**	-	0.25	.01	–	effective mass (in units of m_0) for trap-assisted tunneling of bottom component
29	**MEFFTATSTI**	-	0.25	.01	–	effective mass (in units of m_0) for trap-assisted tunneling of STI-edge component
30	**MEFFTATGAT**	-	0.25	.01	–	effective mass (in units of m_0) for trap-assisted tunneling of gate-edge component

No.	Name	Unit	Default	Min.	Max.	Description
			Band-to-band tunneling parameters			
31	**CBBTBOT**	AV^{-3}	1×10^{-12}	0	–	band-to-band tunneling prefactor of bottom component
32	**CBBTSTI**	$AV^{-3}m$	1×10^{-18}	0	–	band-to-band tunneling prefactor of STI-edge component
33	**CBBTGAT**	$AV^{-3}m$	1×10^{-18}	0	–	band-to-band tunneling prefactor of gate-edge component
34	**FBBTRBOT**	Vm^{-1}	1×10^{9}	–	–	normalization field at the reference temperature for band-to-band tunneling of bottom component
35	**FBBTRSTI**	Vm^{-1}	1×10^{9}	–	–	normalization field at the reference temperature for band-to-band tunneling of STI-edge component
36	**FBBTRGAT**	Vm^{-1}	1×10^{9}	–	–	normalization field at the reference temperature for band-to-band tunneling of gate-edge component
37	**STFBBTBOT**	K^{-1}	-1×10^{-3}	–	–	temperature scaling parameter for band-to-band tunneling of bottom component
38	**STFBBTSTI**	K^{-1}	-1×10^{-3}	–	–	temperature scaling parameter for band-to-band tunneling of STI-edge component
39	**STFBBTGAT**	K^{-1}	-1×10^{-3}	–	–	temperature scaling parameter for band-to-band tunneling of gate-edge component
			Avalanche and breakdown parameters			
40	**VBRBOT**	V	10	0.1	–	breakdown voltage of bottom component
41	**VBRSTI**	V	10	0.1	–	breakdown voltage of STI-edge component
42	**VBRGAT**	V	10	0.1	–	breakdown voltage of gate-edge component
43	**PBRBOT**	V	4	0.1	–	breakdown onset tuning parameter of bottom component
44	**PBRSTI**	V	4	0.1	–	breakdown onset tuning parameter of STI-edge component
45	**PBRGAT**	V	4	0.1	–	breakdown onset tuning parameter of gate-edge component

4 Model equations

4.1 The juncap function

This section describes a function which contains the full characteristics of the JUNCAP2 model. In the actual model it will be called three times: for the bottom, STI-edge, and gate-edge components of the model. It uses the so-called hyp-functions, which are described seperately in section 4.3.

Input parameters of the juncap function

No.	Name	Description
0	$V_{\rm AK}$	in case $\mathbf{TYPE} = 1$: voltage between anode (p-side) and cathode (n-side); in case $\mathbf{TYPE} = -1$: voltage between cathode and anode
1	$T_{\rm KR}$	reference temperature in Kelvin
2	$T_{\rm KD}$	device temperature in Kelvin
3	$\phi_{\rm TD}$	thermal voltage at device temperature
4	$\phi_{\rm GD}$	bandgap voltage at device temperature
5	$F_{\rm TD}$	intrinsic carrier concentration at device temperature, divided by that at reference temperature
6	$I_{\rm DSAT}$	saturation current density of ideal current
7	$V_{\rm bi}$	built-in voltage at the device temperature
8	$V_{\rm bi,min}$	minimum $V_{\rm bi}$ of bottom, STI-edge, and gate-edge contribution
9	$V_{\rm F,min}$	limiting voltage for charge model
10	$V_{\rm ch}$	smoothing constant for transition $V_{\rm F,min} \to V_{\rm ch}$ in charge model
11	$\mathbf{VMAX}$	maximum voltage up to which forward current behaves exponentially
12	$\mathbf{CJOR}$	zero-bias capacitance per unit-of-area
13	$\mathbf{VBIR}$	built-in voltage at the reference temperature
14	$\mathbf{P}$	grading coefficient
15	$\mathbf{CSRH}$	Shockley-Read-Hall prefactor
16	$\mathbf{XJUN}$	junction depth
17	$\mathbf{CTAT}$	trap-assisted tunneling prefactor
18	$\mathbf{MEFFTAT}$	effective mass (in units of m_0) for trap-assisted tunneling
19	$\mathbf{CBBT}$	band-to-band tunneling prefactor
20	$\mathbf{FBBTR}$	normalization field at the reference temperature for band-to-band tunneling
21	$\mathbf{STFBBT}$	temperature scaling parameter for band-to-band tunneling
22	$\mathbf{VBR}$	breakdown voltage
23	$\mathbf{PBR}$	breakdown onset tuning parameter

Outputs of the juncap function

No.	Name	Description
0	I'_j	junction current per unit of area or length
1	Q'_j	junction charge per unit of area or length

Junction charge

$$C_\mathrm{jo} = \mathbf{CJOR} \cdot \left(\frac{\mathbf{VBIR}}{V_\mathrm{bi}}\right)^{\mathbf{P}} \tag{4.1}$$

$$V_\mathrm{j} = \mathrm{hyp}_5(V_\mathrm{AK}; V_\mathrm{F,min}, V_\mathrm{ch}) \tag{4.2}$$

$$Q'_\mathrm{j} = \left\{\frac{C_\mathrm{jo} \cdot V_\mathrm{bi}}{1 - \mathbf{P}} \cdot \left[1 - \left(1 - \frac{V_\mathrm{j}}{V_\mathrm{bi}}\right)^{1-\mathbf{P}}\right] + a \cdot C_\mathrm{jo} \cdot (V_\mathrm{AK} - V_\mathrm{j})\right\} \tag{4.3}$$

Ideal current

$$M_\mathrm{ID} = \begin{cases} \exp\left(\dfrac{V_\mathrm{AK}}{\phi_\mathrm{TD}}\right) & \text{if } V_\mathrm{AK} < V_\mathrm{max} \\ \left(1 + \dfrac{V_\mathrm{AK} - \mathbf{VMAX}}{\phi_\mathrm{TD}}\right) \cdot \exp\left(\dfrac{\mathbf{VMAX}}{\phi_\mathrm{TD}}\right) & \text{if } V_\mathrm{AK} \geq V_\mathrm{max} \end{cases} \tag{4.4}$$

$$I'_\mathrm{D} = (M_\mathrm{ID} - 1) \cdot I_\mathrm{DSAT} \tag{4.5}$$

Shockley-Read-Hall current

Note: if $\mathbf{CSRH} = \mathbf{CTAT} = 0$, Eqs. (4.6)... (4.15) should be skipped and $I'_\mathrm{SRH} = 0$.

$$z_\mathrm{inv} = \sqrt{M_\mathrm{ID}} \tag{4.6}$$

$$z = \frac{1}{z_\mathrm{inv}} \tag{4.7}$$

$$\psi^* = \begin{cases} \phi_\mathrm{TD} \cdot \ln\left[z + 2 + \sqrt{(z+1)\cdot(z+3)}\right] & \text{if } V_\mathrm{AK} > 0 \\ \dfrac{-V_\mathrm{AK}}{2} + \phi_\mathrm{TD} \cdot \ln\left[1 + 2 \cdot z_\mathrm{inv} + \sqrt{(1 + z_\mathrm{inv}) \cdot (1 + 3 \cdot z_\mathrm{inv})}\right] & \text{if } V_\mathrm{AK} \leq 0 \end{cases} \tag{4.8}$$

$$V_\mathrm{j,lim} = V_\mathrm{bi,min} - 2 \cdot \psi^* \tag{4.9}$$

$$V_\mathrm{j,SRH} = \mathrm{hyp}_2(V_\mathrm{AK}; V_\mathrm{j,lim}, \phi_\mathrm{TD}) \tag{4.10}$$

$$w_{\mathrm{SRH,step}} = 1 - \sqrt{1 - \frac{2 \cdot \psi^*}{V_{\mathrm{bi}} - V_{\mathrm{j,SRH}}}} \tag{4.11}$$

$$\Delta w_{\mathrm{SRH}} = \left(\frac{{w_{\mathrm{SRH,step}}}^2 \cdot \ln w_{\mathrm{SRH,step}}}{1 - w_{\mathrm{SRH,step}}} + w_{\mathrm{SRH,step}} \right) \cdot (1 - 2 \cdot \mathbf{P}) \tag{4.12}$$

$$w_{\mathrm{SRH}} = w_{\mathrm{SRH,step}} + \Delta w_{\mathrm{SRH}} \tag{4.13}$$

$$W_{\mathrm{dep}} = \frac{\mathbf{XJUN} \cdot \epsilon_{\mathrm{Si}}}{\mathbf{CJOR}} \cdot \left(\frac{V_{\mathrm{bi}} - V_{\mathrm{j,SRH}}}{\mathbf{VBIR}} \right)^{\mathbf{P}} \tag{4.14}$$

$$I'_{\mathrm{SRH}} = \mathbf{CSRH} \cdot F_{\mathrm{TD}} \cdot (z_{\mathrm{inv}} - 1) \cdot w_{\mathrm{SRH}} \cdot W_{\mathrm{dep}} \tag{4.15}$$

Trap-assisted-tunneling current

Note: if $\mathbf{CTAT} = 0$, Eqs. (4.16)... (4.30) should be skipped and $I'_{\mathrm{TAT}} = 0$.

$$F_{\mathrm{max}} = \frac{V_{\mathrm{bi}} - V_{\mathrm{j,SRH}}}{W_{\mathrm{dep}} \cdot (1 - \mathbf{P})} \tag{4.16}$$

$$m_{\mathrm{eff}} = \mathbf{MEFFTAT} \cdot m_0 \tag{4.17}$$

$$\Delta E = \max\left(\frac{\phi_{\mathrm{GD}}}{2}, \phi_{\mathrm{TD}} \right) \tag{4.18}$$

$$a_{\mathrm{TAT}} = \frac{\Delta E}{\phi_{\mathrm{TD}}} \tag{4.19}$$

$$b_{\mathrm{TAT}} = \frac{\sqrt{32 \cdot m_{\mathrm{eff}} \cdot q \cdot \Delta E^3}}{3 \cdot \hbar \cdot F_{\mathrm{max}}} \tag{4.20}$$

$$u'_{\mathrm{max}} = \left(\frac{2 \cdot a_{\mathrm{TAT}}}{3 \cdot b_{\mathrm{TAT}}} \right)^2 \tag{4.21}$$

$$u_{\mathrm{max}} = \sqrt{\frac{{u'_{\mathrm{max}}}^2}{{u'_{\mathrm{max}}}^2 + 1}} \tag{4.22}$$

$$w_{\Gamma} = \left(1 + b_{\mathrm{TAT}} \cdot {u_{\mathrm{max}}}^{3/2} \right)^{\frac{\mathbf{P}}{\mathbf{P}-1}} \tag{4.23}$$

$$w_{\mathrm{TAT}} = \frac{w_{\mathrm{SRH}} \cdot w_{\Gamma}}{w_{\mathrm{SRH}} + w_{\Gamma}} \tag{4.24}$$

$$k_{\mathrm{TAT}} = \sqrt{\frac{3 \cdot b_{\mathrm{TAT}}}{8 \cdot \sqrt{u_{\mathrm{max}}}}} \tag{4.25}$$

$$l_{\mathrm{TAT}} = \frac{4 \cdot a_{\mathrm{TAT}}}{3 \cdot b_{\mathrm{TAT}}} \cdot \sqrt{u_{\mathrm{max}}} - u_{\mathrm{max}} \tag{4.26}$$

$$m_{\mathrm{TAT}} = \frac{2 \cdot {a_{\mathrm{TAT}}}^2}{3 \cdot b_{\mathrm{TAT}}} \cdot \sqrt{u_{\mathrm{max}}} - a_{\mathrm{TAT}} \cdot u_{\mathrm{max}} + \frac{b_{\mathrm{TAT}}}{2} \cdot {u_{\mathrm{max}}}^{3/2} \tag{4.27}$$

$$\mathrm{erfcapprox}(y) = \begin{cases} t_{\mathrm{erfc}} = \begin{cases} \dfrac{1}{1 + p_{\mathrm{erfc}} \cdot y} & \text{if } y > 0 \\ \dfrac{1}{1 - p_{\mathrm{erfc}} \cdot y} & \text{if } y \leq 0 \end{cases} \\ \mathrm{erfcapprox}^+ = \left(a_{\mathrm{erfc}} \cdot t_{\mathrm{erfc}} + b_{\mathrm{erfc}} \cdot t_{\mathrm{erfc}}^2 + c_{\mathrm{erfc}} \cdot t_{\mathrm{erfc}}^3\right) \cdot \exp(-y^2) \\ \mathrm{erfcapprox}(y) = \begin{cases} \mathrm{erfcapprox}^+ & \text{if} \quad y > 0 \\ 2 - \mathrm{erfcapprox}^+ & \text{if} \quad y \leq 0 \end{cases} \end{cases} \tag{4.28}$$

$$\Gamma_{\mathrm{max}} = \frac{a_{\mathrm{TAT}} \cdot \exp\left(m_{\mathrm{TAT}}\right) \cdot \mathrm{erfcapprox}\left[k_{\mathrm{TAT}} \cdot \left(l_{\mathrm{TAT}} - 1\right)\right] \cdot \sqrt{\pi}}{2 \cdot k_{\mathrm{TAT}}} \tag{4.29}$$

$$I'_{\mathrm{TAT}} = \mathbf{CTAT} \cdot F_{\mathrm{TD}} \cdot (z_{\mathrm{inv}} - 1) \cdot \Gamma_{\mathrm{max}} \cdot w_{\mathrm{TAT}} \cdot W_{\mathrm{dep}} \tag{4.30}$$

Band-to-band tunneling current

Note: if $\mathbf{CBBT} = 0$, Eqs. (4.31)... (4.34) should be skipped and $I'_{\mathrm{BBT}} = 0$.

$$W_{\mathrm{dep,r}} = \frac{\mathbf{XJUN} \cdot \epsilon_{\mathrm{Si}}}{\mathbf{CJOR}} \cdot \left(\frac{\mathbf{VBIR} - V_{\mathrm{j}}}{\mathbf{VBIR}}\right)^{\mathbf{P}} \tag{4.31}$$

$$F_{\mathrm{max,r}} = \frac{\mathbf{VBIR} - V_{\mathrm{j}}}{W_{\mathrm{dep,r}} \cdot (1 - \mathbf{P})} \tag{4.32}$$

$$F_{\mathrm{BBT}} = \mathbf{FBBTR} \cdot [1 + \mathbf{STFBBT} \cdot (T_{\mathrm{KD}} - T_{\mathrm{KR}})] \tag{4.33}$$

$$I'_{\mathrm{BBT}} = \mathbf{CBBT} \cdot V_{\mathrm{AK}} \cdot {F_{\mathrm{max,r}}}^2 \cdot \exp\left(-\frac{F_{\mathrm{BBT}}}{F_{\mathrm{max,r}}}\right) \tag{4.34}$$

Avalanche and breakdown

Note: if $\mathbf{VBR} > V_{\mathrm{br,max}}$, Eqs. (4.35)... (4.38) should be skipped and $f_{\mathrm{breakdown}} = 1$.

$$V_{\mathrm{av}} = \mathrm{hyp}_2(V_{\mathrm{AK}}; 0, \epsilon_{\mathrm{av}}) \tag{4.35}$$

$$f_{\mathrm{stop}} = \frac{1}{1 - {\alpha_{\mathrm{av}}}^{\mathbf{PBR}}} \tag{4.36}$$

$$s_{\mathrm{f}} = -{f_{\mathrm{stop}}}^2 \cdot {\alpha_{\mathrm{av}}}^{\mathbf{PBR}-1} \cdot \frac{\mathbf{PBR}}{\mathbf{VBR}} \tag{4.37}$$

$$f_{\text{breakdown}} = \begin{cases} \dfrac{1}{1 - \left|\dfrac{-V_{\text{av}}}{\mathbf{VBR}}\right|^{\mathbf{PBR}}} & \text{if } V_{\text{av}} > -\alpha_{\text{av}} \cdot \mathbf{VBR} \\ f_{\text{stop}} + (V_{\text{av}} + \alpha_{\text{av}} \cdot \mathbf{VBR}) \cdot s_{\text{f}} & \text{if } V_{\text{av}} \leq -\alpha_{\text{av}} \cdot \mathbf{VBR} \end{cases} \tag{4.38}$$

Total current

$$I'_{\text{j}} = \left(I'_{\text{D}} + I'_{\text{SRH}} + I'_{\text{TAT}} + I'_{\text{BBT}}\right) \cdot f_{\text{breakdown}} \tag{4.39}$$

4.2 The juncap model

Thermal voltage

$$T_{\text{KR}} = T_0 + \mathbf{TRJ} \tag{4.40}$$

$$T_{\text{KD}} = \max(T_0 + T_{\text{A}} + \mathbf{DTA}, T_0 + T_{\text{min}}) \tag{4.41}$$

$$\phi_{\text{TR}} = \frac{k_{\text{B}} \cdot T_{\text{KR}}}{q} \tag{4.42}$$

$$\phi_{\text{TD}} = \frac{k_{\text{B}} \cdot T_{\text{KD}}}{q} \tag{4.43}$$

Band gap

$$\Delta\phi_{\text{GR}} = -\frac{7.02 \cdot 10^{-4} \cdot T_{\text{KR}}^2}{1108.0 + T_{\text{KR}}} \tag{4.44}$$

$$\phi_{\text{GR,bot}} = \mathbf{PHIGBOT} + \Delta\phi_{\text{GR}} \tag{4.45}$$

$$\phi_{\text{GR,sti}} = \mathbf{PHIGSTI} + \Delta\phi_{\text{GR}} \tag{4.46}$$

$$\phi_{\text{GR,gat}} = \mathbf{PHIGGAT} + \Delta\phi_{\text{GR}} \tag{4.47}$$

$$\Delta\phi_{\text{GD}} = -\frac{7.02 \cdot 10^{-4} \cdot T_{\text{KD}}^2}{1108.0 + T_{\text{KD}}} \tag{4.48}$$

$$\phi_{\text{GD,bot}} = \mathbf{PHIGBOT} + \Delta\phi_{\text{GD}} \tag{4.49}$$

$$\phi_{\text{GD,sti}} = \mathbf{PHIGSTI} + \Delta\phi_{\text{GD}} \tag{4.50}$$

$$\phi_{\text{GD,gat}} = \mathbf{PHIGGAT} + \Delta\phi_{\text{GD}} \tag{4.51}$$

Intrinsic carrier concentration

$$F_{\mathrm{TD,bot}} = \left(\frac{T_{\mathrm{KD}}}{T_{\mathrm{KR}}}\right)^{1.5} \cdot \exp\left(\frac{\phi_{\mathrm{GR,bot}}}{2\cdot\phi_{\mathrm{TR}}} - \frac{\phi_{\mathrm{GD,bot}}}{2\cdot\phi_{\mathrm{TD}}}\right) \tag{4.52}$$

$$F_{\mathrm{TD,sti}} = \left(\frac{T_{\mathrm{KD}}}{T_{\mathrm{KR}}}\right)^{1.5} \cdot \exp\left(\frac{\phi_{\mathrm{GR,sti}}}{2\cdot\phi_{\mathrm{TR}}} - \frac{\phi_{\mathrm{GD,sti}}}{2\cdot\phi_{\mathrm{TD}}}\right) \tag{4.53}$$

$$F_{\mathrm{TD,gat}} = \left(\frac{T_{\mathrm{KD}}}{T_{\mathrm{KR}}}\right)^{1.5} \cdot \exp\left(\frac{\phi_{\mathrm{GR,gat}}}{2\cdot\phi_{\mathrm{TR}}} - \frac{\phi_{\mathrm{GD,gat}}}{2\cdot\phi_{\mathrm{TD}}}\right) \tag{4.54}$$

Saturation current density at device temperature

$$I_{\mathrm{DSAT,bot}} = \mathbf{IDSATRBOT} \cdot {F_{\mathrm{TD,bot}}}^2 \tag{4.55}$$

$$I_{\mathrm{DSAT,sti}} = \mathbf{IDSATRSTI} \cdot {F_{\mathrm{TD,sti}}}^2 \tag{4.56}$$

$$I_{\mathrm{DSAT,gat}} = \mathbf{IDSATRGAT} \cdot {F_{\mathrm{TD,gat}}}^2 \tag{4.57}$$

Determination of V_{max}

$$V_{\mathrm{max,bot}} = \begin{cases} V_{\mathrm{max,large}} & \text{if } I_{\mathrm{DSAT,bot}} \cdot \mathbf{AB} = 0 \\ \phi_{\mathrm{TD}} \cdot \ln\left(\dfrac{\mathbf{IMAX}}{I_{\mathrm{DSAT,bot}} \cdot \mathbf{AB}} + 1\right) & \text{if } I_{\mathrm{DSAT,bot}} \cdot \mathbf{AB} \neq 0 \end{cases} \tag{4.58}$$

$$V_{\mathrm{max,sti}} = \begin{cases} V_{\mathrm{max,large}} & \text{if } I_{\mathrm{DSAT,sti}} \cdot \mathbf{LS} = 0 \\ \phi_{\mathrm{TD}} \cdot \ln\left(\dfrac{\mathbf{IMAX}}{I_{\mathrm{DSAT,sti}} \cdot \mathbf{LS}} + 1\right) & \text{if } I_{\mathrm{DSAT,sti}} \cdot \mathbf{LS} \neq 0 \end{cases} \tag{4.59}$$

$$V_{\mathrm{max,gat}} = \begin{cases} V_{\mathrm{max,large}} & \text{if } I_{\mathrm{DSAT,gat}} \cdot \mathbf{LG} = 0 \\ \phi_{\mathrm{TD}} \cdot \ln\left(\dfrac{\mathbf{IMAX}}{I_{\mathrm{DSAT,gat}} \cdot \mathbf{LG}} + 1\right) & \text{if } I_{\mathrm{DSAT,gat}} \cdot \mathbf{LG} \neq 0 \end{cases} \tag{4.60}$$

$$V_{\mathrm{max}} = \min\left(V_{\mathrm{max,bot}}, V_{\mathrm{max,sti}}, V_{\mathrm{max,gat}}\right) \tag{4.61}$$

Built-in voltages

$$U_{\mathrm{bi,bot}} = \mathbf{VBIRBOT} \cdot \frac{T_{\mathrm{KD}}}{T_{\mathrm{KR}}} - 2 \cdot \phi_{\mathrm{TD}} \cdot \ln F_{\mathrm{TD,bot}} \tag{4.62}$$

$$V_{\mathrm{bi,bot}} = U_{\mathrm{bi,bot}} + \phi_{\mathrm{TD}} \cdot \ln\left[1 + \exp\left(\frac{V_{\mathrm{bi,low}} - U_{\mathrm{bi,bot}}}{\phi_{\mathrm{TD}}}\right)\right] \tag{4.63}$$

$$U_{\mathrm{bi,sti}} = \mathbf{VBIRSTI} \cdot \frac{T_{\mathrm{KD}}}{T_{\mathrm{KR}}} - 2 \cdot \phi_{\mathrm{TD}} \cdot \ln F_{\mathrm{TD,sti}} \tag{4.64}$$

$$V_{\mathrm{bi,sti}} = U_{\mathrm{bi,sti}} + \phi_{\mathrm{TD}} \cdot \ln \left[1 + \exp \left(\frac{V_{\mathrm{bi,low}} - U_{\mathrm{bi,sti}}}{\phi_{\mathrm{TD}}} \right) \right] \tag{4.65}$$

$$U_{\mathrm{bi,gat}} = \mathbf{VBIRGAT} \cdot \frac{T_{\mathrm{KD}}}{T_{\mathrm{KR}}} - 2 \cdot \phi_{\mathrm{TD}} \cdot \ln F_{\mathrm{TD,gat}} \tag{4.66}$$

$$V_{\mathrm{bi,gat}} = U_{\mathrm{bi,gat}} + \phi_{\mathrm{TD}} \cdot \ln \left[1 + \exp \left(\frac{V_{\mathrm{bi,low}} - U_{\mathrm{bi,gat}}}{\phi_{\mathrm{TD}}} \right) \right] \tag{4.67}$$

Determination of $V_{\mathrm{F,min}}$ and V_{ch}

$$V_{\mathrm{bi,min}} = \min \left(V_{\mathrm{bi,bot}}, V_{\mathrm{bi,sti}}, V_{\mathrm{bi,gat}} \right) \tag{4.68}$$

Note: in taking this minimum, only the V_{bi} of the relevant contributions are taken into account. For example, when $\mathbf{AB} = 0$, $V_{\mathrm{bi,bot}}$ is not taken into account.

$$V_{\mathrm{F,min}} = \begin{cases} V_{\mathrm{bi,min}} \cdot \left(1 - a^{-1/\mathbf{PBOT}} \right) & \text{if } V_{\mathrm{bi,min}} = V_{\mathrm{bi,bot}} \\ V_{\mathrm{bi,min}} \cdot \left(1 - a^{-1/\mathbf{PSTI}} \right) & \text{if } V_{\mathrm{bi,min}} = V_{\mathrm{bi,sti}} \\ V_{\mathrm{bi,min}} \cdot \left(1 - a^{-1/\mathbf{PGAT}} \right) & \text{if } V_{\mathrm{bi,min}} = V_{\mathrm{bi,gat}} \end{cases} \tag{4.69}$$

$$V_{\mathrm{ch}} = \epsilon_{\mathrm{ch}} \cdot V_{\mathrm{bi,min}} \tag{4.70}$$

Voltage difference V_{AK}

$$V_{\mathrm{AK}} = \mathbf{TYPE} \cdot (V_{\mathrm{A}} - V_{\mathrm{K}}) \tag{4.71}$$

4.2.1 Junction charge

$$\begin{aligned} Q'_{\mathrm{j,bot}} = \; & Q'_{\mathrm{j}} (V_{\mathrm{AK}} = V_{\mathrm{AK}}, \; T_{\mathrm{KR}} = T_{\mathrm{KR}}, \; T_{\mathrm{KD}} = T_{\mathrm{KD}}, \; \phi_{\mathrm{TD}} = \phi_{\mathrm{TD}}, \\ & \phi_{\mathrm{GR}} = \phi_{\mathrm{GR,bot}}, \; \phi_{\mathrm{GD}} = \phi_{\mathrm{GD,bot}}, \; F_{\mathrm{TD}} = F_{\mathrm{TD,bot}}, \\ & I_{\mathrm{DSAT}} = I_{\mathrm{DSAT,bot}}, \; V_{\mathrm{bi}} = V_{\mathrm{bi,bot}}, \; V_{\mathrm{bi,min}} = V_{\mathrm{bi,min}}, \; V_{\mathrm{F,min}} = V_{\mathrm{F,min}}, \\ & V_{\mathrm{ch}} = V_{\mathrm{ch}}, \; \mathbf{VMAX} = \mathbf{VMAX}, \; \mathbf{CJOR} = \mathbf{CJORBOT}, \\ & \mathbf{VBIR} = \mathbf{VBIRBOT}, \; \mathbf{P} = \mathbf{PBOT}, \; \mathbf{CSRH} = \mathbf{CSRHBOT}, \\ & \mathbf{XJUN} = 1, \; \mathbf{CTAT} = \mathbf{CTATBOT}, \\ & \mathbf{MEFFTAT} = \mathbf{MEFFTATBOT}, \; \mathbf{CBBT} = \mathbf{CBBTBOT}, \\ & \mathbf{FBBTR} = \mathbf{FBBTRBOT}, \; \mathbf{STFBBT} = \mathbf{STFBBTBOT}, \\ & \mathbf{VBR} = \mathbf{VBRBOT}, \; \mathbf{PBR} = \mathbf{PBRBOT} \;) \end{aligned} \tag{4.72}$$

$$
\begin{aligned}
Q'_{\mathrm{j,sti}} \;=\; & Q'_{\mathrm{j}}\,(V_{\mathrm{AK}}=V_{\mathrm{AK}},\ T_{\mathrm{KR}}=T_{\mathrm{KR}},\ T_{\mathrm{KD}}=T_{\mathrm{KD}},\ \phi_{\mathrm{TD}}=\phi_{\mathrm{TD}},\\
& \phi_{\mathrm{GR}}=\phi_{\mathrm{GR,sti}}\,,\ \phi_{\mathrm{GD}}=\phi_{\mathrm{GD,sti}}\,,\ F_{\mathrm{TD}}=F_{\mathrm{TD,sti}}\,,\\
& I_{\mathrm{DSAT}}=I_{\mathrm{DSAT,sti}}\,,\ V_{\mathrm{bi}}=V_{\mathrm{bi,sti}}\,,\ V_{\mathrm{bi,min}}=V_{\mathrm{bi,min}}\,,\ V_{\mathrm{F,min}}=V_{\mathrm{F,min}}\,,\\
& V_{\mathrm{ch}}=V_{\mathrm{ch}}\,,\ \mathbf{VMAX}=\mathbf{VMAX},\ \mathbf{CJOR}=\mathbf{CJORSTI},\\
& \mathbf{VBIR}=\mathbf{VBIRSTI},\ \mathbf{P}=\mathbf{PSTI},\ \mathbf{CSRH}=\mathbf{CSRHSTI},\\
& \mathbf{XJUN}=\mathbf{XJUNSTI},\ \mathbf{CTAT}=\mathbf{CTATSTI},\\
& \mathbf{MEFFTAT}=\mathbf{MEFFTATSTI},\ \mathbf{CBBT}=\mathbf{CBBTSTI},\\
& \mathbf{FBBTR}=\mathbf{FBBTRSTI},\ \mathbf{STFBBT}=\mathbf{STFBBTSTI},\\
& \mathbf{VBR}=\mathbf{VBRSTI},\ \mathbf{PBR}=\mathbf{PBRSTI}\ )
\end{aligned}
\tag{4.73}
$$

$$
\begin{aligned}
Q'_{\mathrm{j,gat}} \;=\; & Q'_{\mathrm{j}}\,(V_{\mathrm{AK}}=V_{\mathrm{AK}},\ T_{\mathrm{KR}}=T_{\mathrm{KR}},\ T_{\mathrm{KD}}=T_{\mathrm{KD}},\ \phi_{\mathrm{TD}}=\phi_{\mathrm{TD}},\\
& \phi_{\mathrm{GR}}=\phi_{\mathrm{GR,gat}}\,,\ \phi_{\mathrm{GD}}=\phi_{\mathrm{GD,gat}}\,,\ F_{\mathrm{TD}}=F_{\mathrm{TD,gat}}\,,\\
& I_{\mathrm{DSAT}}=I_{\mathrm{DSAT,gat}}\,,\ V_{\mathrm{bi}}=V_{\mathrm{bi,gat}}\,,\ V_{\mathrm{bi,min}}=V_{\mathrm{bi,min}}\,,\ V_{\mathrm{F,min}}=V_{\mathrm{F,min}}\,,\\
& V_{\mathrm{ch}}=V_{\mathrm{ch}}\,,\ \mathbf{VMAX}=\mathbf{VMAX},\ \mathbf{CJOR}=\mathbf{CJORGAT},\\
& \mathbf{VBIR}=\mathbf{VBIRGAT},\ \mathbf{P}=\mathbf{PGAT},\ \mathbf{CSRH}=\mathbf{CSRHGAT},\\
& \mathbf{XJUN}=\mathbf{XJUNGAT},\ \mathbf{CTAT}=\mathbf{CTATGAT},\\
& \mathbf{MEFFTAT}=\mathbf{MEFFTATGAT},\ \mathbf{CBBT}=\mathbf{CBBTGAT},\\
& \mathbf{FBBTR}=\mathbf{FBBTRGAT},\ \mathbf{STFBBT}=\mathbf{STFBBTGAT},\\
& \mathbf{VBR}=\mathbf{VBRGAT},\ \mathbf{PBR}=\mathbf{PBRGAT}\ )
\end{aligned}
\tag{4.74}
$$

$$
Q_{\mathrm{j}}=\mathbf{TYPE}\cdot\mathbf{MULT}\cdot\left(\mathbf{AB}\cdot Q'_{\mathrm{j,bot}}+\mathbf{LS}\cdot Q'_{\mathrm{j,sti}}+\mathbf{LG}\cdot Q'_{\mathrm{j,gat}}\right)
\tag{4.75}
$$

4.2.2 Junction current

$$
\begin{aligned}
I'_{\mathrm{j,bot}} \;=\; & I'_{\mathrm{j}}\,(V_{\mathrm{AK}}=V_{\mathrm{AK}},\ T_{\mathrm{KR}}=T_{\mathrm{KR}},\ T_{\mathrm{KD}}=T_{\mathrm{KD}},\ \phi_{\mathrm{TD}}=\phi_{\mathrm{TD}},\\
& \phi_{\mathrm{GR}}=\phi_{\mathrm{GR,bot}}\,,\ \phi_{\mathrm{GD}}=\phi_{\mathrm{GD,bot}}\,,\ F_{\mathrm{TD}}=F_{\mathrm{TD,bot}}\,,\\
& I_{\mathrm{DSAT}}=I_{\mathrm{DSAT,bot}}\,,\ V_{\mathrm{bi}}=V_{\mathrm{bi,bot}}\,,\ V_{\mathrm{bi,min}}=V_{\mathrm{bi,min}}\,,\ V_{\mathrm{F,min}}=V_{\mathrm{F,min}}\,,\\
& V_{\mathrm{ch}}=V_{\mathrm{ch}}\,,\ \mathbf{VMAX}=\mathbf{VMAX},\ \mathbf{CJOR}=\mathbf{CJORBOT},\\
& \mathbf{VBIR}=\mathbf{VBIRBOT},\ \mathbf{P}=\mathbf{PBOT},\ \mathbf{CSRH}=\mathbf{CSRHBOT},\\
& \mathbf{XJUN}=1,\ \mathbf{CTAT}=\mathbf{CTATBOT},\\
& \mathbf{MEFFTAT}=\mathbf{MEFFTATBOT},\ \mathbf{CBBT}=\mathbf{CBBTBOT},\\
& \mathbf{FBBTR}=\mathbf{FBBTRBOT},\ \mathbf{STFBBT}=\mathbf{STFBBTBOT},\\
& \mathbf{VBR}=\mathbf{VBRBOT},\ \mathbf{PBR}=\mathbf{PBRBOT}\ )
\end{aligned}
\tag{4.76}
$$

$$
\begin{aligned}
I'_{\mathrm{j,sti}} \;=\; & I'_{\mathrm{j}}\,(V_{\mathrm{AK}} = V_{\mathrm{AK}},\;\; T_{\mathrm{KR}} = T_{\mathrm{KR}},\;\; T_{\mathrm{KD}} = T_{\mathrm{KD}},\;\; \phi_{\mathrm{TD}} = \phi_{\mathrm{TD}}, \\
& \phi_{\mathrm{GR}} = \phi_{\mathrm{GR,sti}}\,,\;\; \phi_{\mathrm{GD}} = \phi_{\mathrm{GD,sti}}\,,\;\; F_{\mathrm{TD}} = F_{\mathrm{TD,sti}}\,, \\
& I_{\mathrm{DSAT}} = I_{\mathrm{DSAT,sti}}\,,\;\; V_{\mathrm{bi}} = V_{\mathrm{bi,sti}}\,,\;\; V_{\mathrm{bi,min}} = V_{\mathrm{bi,min}}\,,\;\; V_{\mathrm{F,min}} = V_{\mathrm{F,min}}\,, \\
& V_{\mathrm{ch}} = V_{\mathrm{ch}}\,,\;\; \mathbf{VMAX} = \mathbf{VMAX},\;\; \mathbf{CJOR} = \mathbf{CJORSTI}, \\
& \mathbf{VBIR} = \mathbf{VBIRSTI},\;\; \mathbf{P} = \mathbf{PSTI},\;\; \mathbf{CSRH} = \mathbf{CSRHSTI}, \\
& \mathbf{XJUN} = \mathbf{XJUNSTI},\;\; \mathbf{CTAT} = \mathbf{CTATSTI}, \\
& \mathbf{MEFFTAT} = \mathbf{MEFFTATSTI},\;\; \mathbf{CBBT} = \mathbf{CBBTSTI}, \\
& \mathbf{FBBTR} = \mathbf{FBBTRSTI},\;\; \mathbf{STFBBT} = \mathbf{STFBBTSTI}, \\
& \mathbf{VBR} = \mathbf{VBRSTI},\;\; \mathbf{PBR} = \mathbf{PBRSTI}\;\;)
\end{aligned} \tag{4.77}
$$

$$
\begin{aligned}
I'_{\mathrm{j,gat}} \;=\; & I'_{\mathrm{j}}\,(V_{\mathrm{AK}} = V_{\mathrm{AK}},\;\; T_{\mathrm{KR}} = T_{\mathrm{KR}},\;\; T_{\mathrm{KD}} = T_{\mathrm{KD}},\;\; \phi_{\mathrm{TD}} = \phi_{\mathrm{TD}}, \\
& \phi_{\mathrm{GR}} = \phi_{\mathrm{GR,gat}}\,,\;\; \phi_{\mathrm{GD}} = \phi_{\mathrm{GD,gat}}\,,\;\; F_{\mathrm{TD}} = F_{\mathrm{TD,gat}}\,, \\
& I_{\mathrm{DSAT}} = I_{\mathrm{DSAT,gat}}\,,\;\; V_{\mathrm{bi}} = V_{\mathrm{bi,gat}}\,,\;\; V_{\mathrm{bi,min}} = V_{\mathrm{bi,min}}\,,\;\; V_{\mathrm{F,min}} = V_{\mathrm{F,min}}\,, \\
& V_{\mathrm{ch}} = V_{\mathrm{ch}}\,,\;\; \mathbf{VMAX} = \mathbf{VMAX},\;\; \mathbf{CJOR} = \mathbf{CJORGAT}, \\
& \mathbf{VBIR} = \mathbf{VBIRGAT},\;\; \mathbf{P} = \mathbf{PGAT},\;\; \mathbf{CSRH} = \mathbf{CSRHGAT}, \\
& \mathbf{XJUN} = \mathbf{XJUNGAT},\;\; \mathbf{CTAT} = \mathbf{CTATGAT}, \\
& \mathbf{MEFFTAT} = \mathbf{MEFFTATGAT},\;\; \mathbf{CBBT} = \mathbf{CBBTGAT}, \\
& \mathbf{FBBTR} = \mathbf{FBBTRGAT},\;\; \mathbf{STFBBT} = \mathbf{STFBBTGAT}, \\
& \mathbf{VBR} = \mathbf{VBRGAT},\;\; \mathbf{PBR} = \mathbf{PBRGAT}\;\;)
\end{aligned} \tag{4.78}
$$

$$
I_{\mathrm{j}} = \mathbf{TYPE} \cdot \mathbf{MULT} \cdot \left(\mathbf{AB} \cdot I'_{\mathrm{j,bot}} + \mathbf{LS} \cdot I'_{\mathrm{j,sti}} + \mathbf{LG} \cdot I'_{\mathrm{j,gat}} \right) \tag{4.79}
$$

4.2.3 Junction noise

$$
S_{\mathrm{I}} = 2 \cdot q \cdot |I_{\mathrm{j}}| \tag{4.80}
$$

4.3 Auxiliary equations

In this section, the *hyp*-functions that are used in the JUNCAP model equations are defined. These functions have been adopted from MOS Model 9, and their naming is consistent with the MOS Model 9 description [4]. The functions hyp_1, hyp_2, and hyp_5 are given by Eqs. (4.81), (4.82), and (4.83), respectively, and illustrated in Figs. 4.1, 4.2, and 4.3, respectively.

$$
\mathrm{hyp}_1(x;\epsilon) = \frac{1}{2} \cdot \left(x + \sqrt{x^2 + 4 \cdot \epsilon^2} \right) \tag{4.81}
$$

$$
\mathrm{hyp}_2(x;x_0,\epsilon) = x - \mathrm{hyp}_1(x - x_0;\epsilon) \tag{4.82}
$$

$$
\mathrm{hyp}_5(x;x_0,\epsilon) = x_0 - \mathrm{hyp}_1(x_0 - x - \frac{\epsilon^2}{x_0};\epsilon) \tag{4.83}
$$

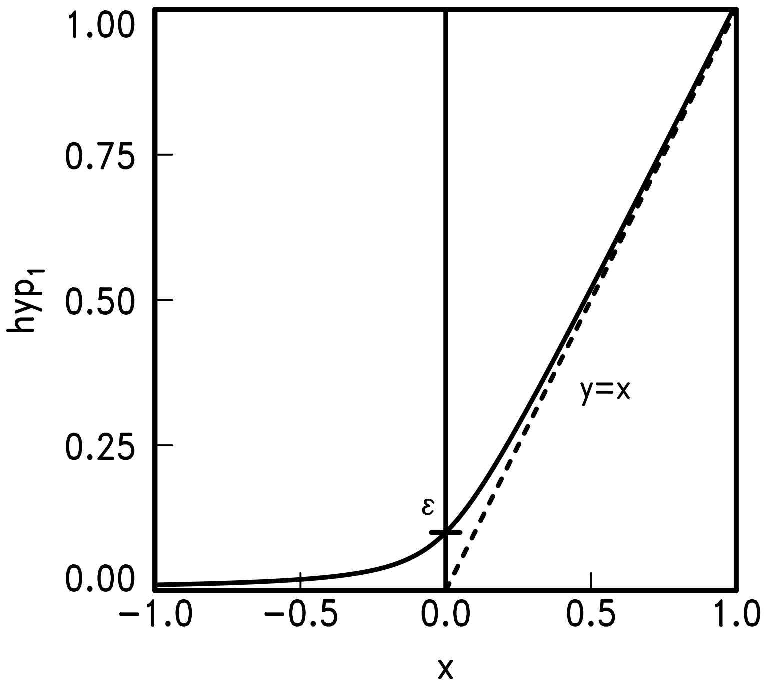

Figure 4.1: The hyp_1 function.

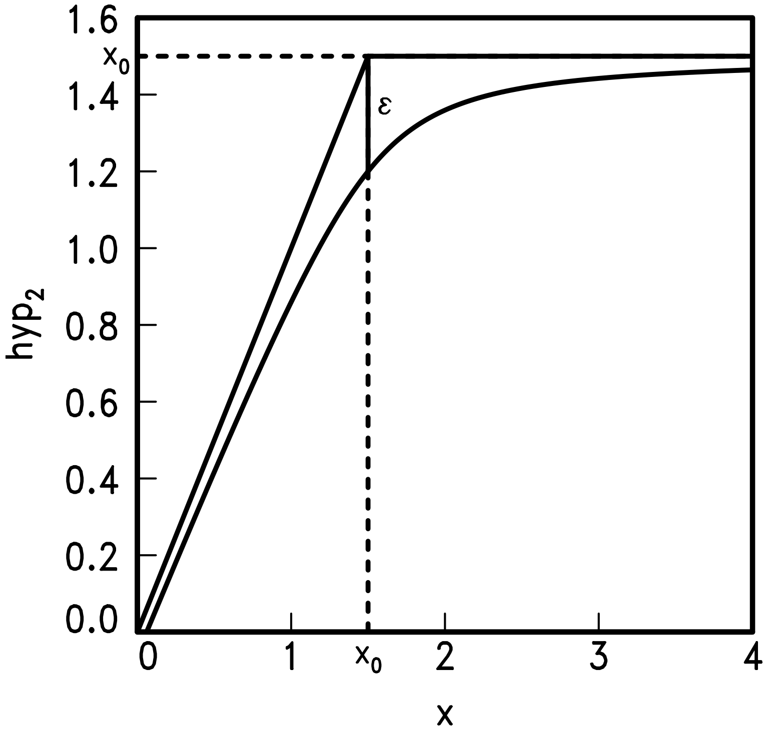

Figure 4.2: The hyp_2 function.

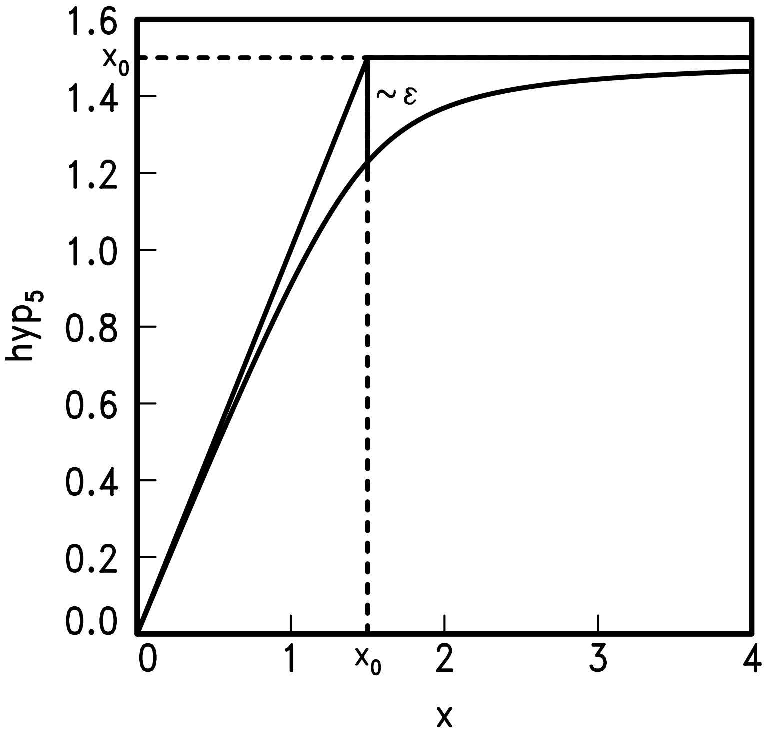

Figure 4.3: The hyp_5 function.

5 DC operating point output

The DC operating point output facility gives information on the state of a device at its operating point.

No.	Name	Unit	Value	Description
0	$\mathbf{VAK}$	V	$\mathbf{TYPE} \cdot V_{\mathrm{AK}}$	voltage between anode and cathode
1	$\mathbf{CJ}$	F	$\dfrac{\partial Q_{\mathrm{j}}}{\partial V_{\mathrm{AK}}}$	total junction capacitance
2	$\mathbf{CJBOT}$	F	$\mathbf{TYPE} \cdot \mathbf{MULT} \cdot \mathbf{AB} \cdot \dfrac{\partial Q'_{\mathrm{j,bot}}}{\partial V_{\mathrm{AK}}}$	bottom component of the junction capacitance
3	$\mathbf{CJSTI}$	F	$\mathbf{TYPE} \cdot \mathbf{MULT} \cdot \mathbf{LS} \cdot \dfrac{\partial Q'_{\mathrm{j,sti}}}{\partial V_{\mathrm{AK}}}$	STI-edge component of the junction capacitance
4	$\mathbf{CJGAT}$	F	$\mathbf{TYPE} \cdot \mathbf{MULT} \cdot \mathbf{LG} \cdot \dfrac{\partial Q'_{\mathrm{j,gat}}}{\partial V_{\mathrm{AK}}}$	gate-edge component of the junction capacitance
5	$\mathbf{IJ}$	A	I_{j}	total junction current
6	$\mathbf{IJBOT}$	A	$\mathbf{TYPE} \cdot \mathbf{MULT} \cdot \mathbf{AB} \cdot I'_{\mathrm{j,bot}}$	bottom component of the junction current
7	$\mathbf{IJSTI}$	A	$\mathbf{TYPE} \cdot \mathbf{MULT} \cdot \mathbf{LS} \cdot I'_{\mathrm{j,sti}}$	STI-edge component of the junction current
8	$\mathbf{IJGAT}$	A	$\mathbf{TYPE} \cdot \mathbf{MULT} \cdot \mathbf{LG} \cdot I'_{\mathrm{j,gat}}$	gate-edge component of the junction current
9	$\mathbf{SI}$	A^2/Hz	S_{I}	total junction current noise spectral density

6 Parameter extraction

6.1 Test structures

For extraction of JUNCAP2 parameters, one needs three different test structures, depicted schematically in Figure 6.1. The first structure is a simple, square diode, which has a large bottom component, a relatively small STI-edge component, and no gate-edge component. The second structure is a finger diode, which has a much larger STI-edge component, and no gate-edge component. The third structure is a Miller diode, which is nothing else than a multi-fingered MOSFET with source and drains tied together. It has a relatively small STI-edge component, and a significant gate-edge component. Besides the three test structures described here, which are needed for parameter extraction, one can optionally use additional geometries for verification purposes. The test structures should be sufficiently large so that currents and capacitances are easily measurable.

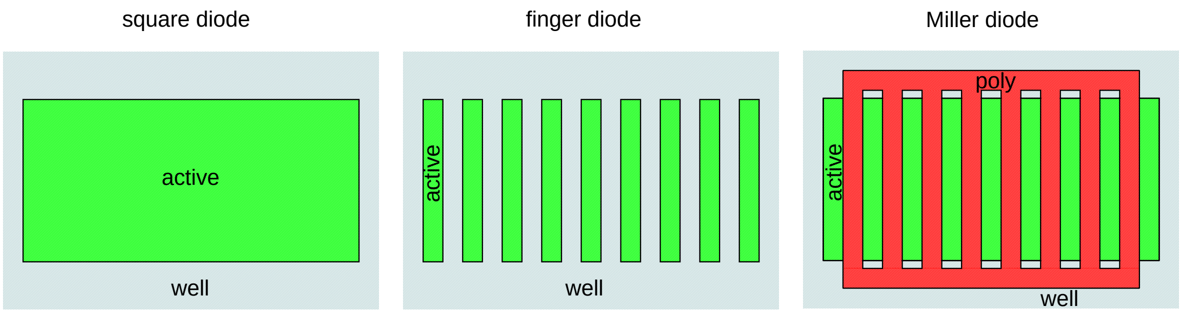

Figure 6.1: Schematic representation of three test structures needed for parameter extraction.

6.2 Measurements

For extraction of JUNCAP2 parameters, one needs both CV and IV measurements. The IV data should be taken over a large range of temperatures, ranging from -40 °C to at least 125 °C. If available, even higher temperatures can be very helpful in the extraction because the junction current tends more and more to ideal behavior at higher temperatures.

Because the temperature dependence of capacitance is fairly low, it is possible (but not recommended) to restrict oneself to room-temperature CV measurements only. For optimal accuracy of the capacitance model however, measurements at different temperature are needed. Therefore it is recommended to take the CV data at the same temperatures as the IV data.

All IV measurements should be done from reverse bias ($-V_{\mathrm{supply}}$) up to small forward bias (e.g. 0.5 V). If avalanche breakdown parameters need to be extracted, one needs to do additional measurements with a reverse bias much larger than the supply voltage. Because the JUNCAP2 model has no parameters to model temperature dependence of the breakdown, it suffices to do this breakdown characterization at room temperature. In the IV measurements, it is recommended to apply a current compliance (e.g. 10 mA) to avoid damaging the test structures when they are biased in the forward regime or in the avalanche breakdown regime.

The CV measurements should be done from reverse bias ($-V_{\text{supply}}$) up to zero bias. CV measurements in the forward mode of operation rapidly become unreliable because the phase angle starts to deviate from 90° quickly. When the junction capacitance is measured on a Miller diode, the gate should be grounded.

6.3 Extraction of bottom, STI-edge, and gate-edge components

All measurements are carried out on three test structures. The measurements on these three structures are used to extract the three components (bottom, STI-edge, and gate-edge components) of either current or capacitance. For the capacitance, the extraction procedure will be outlined below.

For the capacitance of the square diode and finger diode, both having zero gate edge, we can write:

$$C_{\text{j,square}} = \mathbf{AB}_{\text{square}} \cdot C'_{\text{j,bot}} + \mathbf{LS}_{\text{square}} \cdot C'_{\text{j,sti}} \tag{6.1}$$

$$C_{\text{j,finger}} = \mathbf{AB}_{\text{finger}} \cdot C'_{\text{j,bot}} + \mathbf{LS}_{\text{finger}} \cdot C'_{\text{j,sti}} \tag{6.2}$$

For the Miller diode, we write:

$$C_{\text{j,Miller}} = \mathbf{AB}_{\text{Miller}} \cdot C'_{\text{j,bot}} + \mathbf{LS}_{\text{Miller}} \cdot C'_{\text{j,sti}} + \mathbf{LG}_{\text{Miller}} \cdot C'_{\text{j,gat}} \tag{6.3}$$

From Eqs. (6.1) and (6.2) we straightforwardly solve the two unknowns $C'_{\text{j,bot}}$ and $C'_{\text{j,sti}}$:

$$C'_{\text{j,bot}} = \frac{\mathbf{LS}_{\text{finger}} \cdot C_{\text{j,square}} - \mathbf{LS}_{\text{square}} \cdot C_{\text{j,finger}}}{\mathbf{LS}_{\text{finger}} \cdot \mathbf{AB}_{\text{square}} - \mathbf{LS}_{\text{square}} \cdot \mathbf{AB}_{\text{finger}}} \tag{6.4}$$

$$C'_{\text{j,sti}} = \frac{\mathbf{AB}_{\text{square}} \cdot C_{\text{j,finger}} - \mathbf{AB}_{\text{finger}} \cdot C_{\text{j,square}}}{\mathbf{LS}_{\text{finger}} \cdot \mathbf{AB}_{\text{square}} - \mathbf{LS}_{\text{square}} \cdot \mathbf{AB}_{\text{finger}}} \tag{6.5}$$

And now we can derive the final unknown quantity $C'_{\text{j,gat}}$ from Eq. (6.3):

$$C'_{\text{j,gat}} = \frac{C_{\text{j,Miller}} - \mathbf{AB}_{\text{Miller}} \cdot C'_{\text{j,bot}} - \mathbf{LS}_{\text{Miller}} \cdot C'_{\text{j,sti}}}{\mathbf{LG}_{\text{Miller}}} \tag{6.6}$$

The procedure as outlined above is also applied to the junction currents, resulting in the current components $I'_{\text{j,bot}}$, $I'_{\text{j,sti}}$, and $I'_{\text{j,gat}}$.

6.4 Extraction of CV parameters

Having extracted the current and capacitance components as explained in Section 6.3, we are ready for the actual parameter extraction.

First, one has to set some general parameters:

- **LEVEL** is equal to 200 for the first release of the JUNCAP2 model. Possible successors will be 201, 202, etc.
- **TYPE** should be set properly to select either $n-p$ or $p-n$ junction.

- $\mathbf{DTA}$ should be set to zero
- $\mathbf{IMAX}$ should be set to a value which is large enough (e.g. larger than the highest forward current measured) so that it does not affect the extraction procedure.

Before IV parameter extraction is started, it is mandatory to perform the CV extraction first, because the CV parameters are used throughout the IV model. In other words, changing CV parameters *after* IV parameter extraction will change not only the CV curves, but also the IV curves.

The CV parameter extraction is basically the same for the three components. Therefore we will restrict the description to the bottom component. The $\mathbf{PHIGBOT}$ has to be initialized to a reasonable value, e.g. 1.16 V. (It will be fitted later on to the forward IV curves, but this usually has a negligible effect on the CV curves). If needed, one From the CV curves, one extracts three parameters per component:

- $\mathbf{CJORBOT}$, i.e. the zero-bias capacitance per unit of area at the reference temperature. Its initial value is directly taken from the $C'_{\mathrm{j,bot}}$ curves. One should select the $C'_{\mathrm{j,bot}}$ curve measured at the temperature closest to the reference temperature, and use the zero-bias $C'_{\mathrm{j,bot}}$ value of that curves as starting value for $\mathbf{CJORBOT}$.
- $\mathbf{PBOT}$, i.e. the grading coefficient. As starting value one can take $\mathbf{PBOT} = 0.5$.
- $\mathbf{VBIRBOT}$, i.e. the junction built-in voltage at the reference temperature As starting value one can take $\mathbf{VBIRBOT} = 1$.

Using the starting values specified above, one can perform a least-square fit of these three parameters to the measured CV curves. Typical values for the grading coefficient are between 0.3 and 0.6. Typical values for the built-in voltage are between 0.5 V and 1.2 V (from physics, we know that this quantity may exceed the band gap voltage only slightly).

6.5 Extraction of IV parameters

Ideal-current parameters

The IV parameter extraction starts with the extraction of the ideal-current parameters, which are $\mathbf{IDSATRBOT}$ and $\mathbf{PHIGBOT}$ (we restrict ourselves again to the bottom component). The parameter $\mathbf{IDSATRBOT}$ has effect on the ideal current only. The parameter $\mathbf{PHIGBOT}$ is used throughout the model. The ideal-current parameters are extracted on those parts of the forward IV curves which shown nearly ideal behavior. These parts are selected using the ideality factor n_{bot} which can be determined from the forward IV measurements as follows:

$$n_{\mathrm{bot}} = \phi_{\mathrm{TD}} \cdot \frac{\partial I'_{\mathrm{j,bot}}}{\partial V_{\mathrm{AK}}} \tag{6.7}$$

For the fitting of the ideal-current parameters we select those measurement points, for which the ideality factor is reasonably close to 1. For instance, the criterion $n_{\mathrm{bot}} > 0.9$ works well for this purpose. Because the parameter $\mathbf{PHIGBOT}$ has already been initialized to 1.16, we only need to worry about a starting value for $\mathbf{IDSATRBOT}$. This starting value can be found by setting $\mathbf{IDSATRBOT}$ to 1, and calculate the average ratio of measured and modelled current in the region selected by the ideality-factor method. (Note: this can only be done successfully when $\mathbf{IMAX}$ is temporarily set to a huge value.) After this initialization, modelled and measured curves should be reasonably close and one can further optimize the parameters **IDSATRBOT** and **PHIGBOT** using a least-square fit of the model to the measurement points selected by the ideality-factor method.

Please note once more that this ideality factor is only a quantity directly derived from measurements. It is not a model parameter as in many other junction models.

Identification of leakage mechanisms

The next step is the extraction of the remaining leakage current parameters. First, one needs to get an idea which effects need to be included. Sometimes, only Shockley-Read-Hall and trap-assisted tunneling are relevant, sometimes only band-to-band-tunneling, sometimes both. To this purpose one may investigate the temperature dependence by inspection of the activation energy of the leakage currents, which is calculated (in eV) as follows:

$$E_{\mathrm{act}} = \frac{\partial \ln\left(I'_{\mathrm{j,bot}}\right)}{\partial \phi_{\mathrm{TD}}^{-1}} \tag{6.8}$$

An activation energy close to the bandgap (1.16 eV) is an indication that the current is ideal. An activation energy around half the bandgap is an indication that the current is dominated by Shockley-Read-Hall and trap-assisted tunneling. An activation energy well below half the bandgap is an indication that the current is dominated by band-to-band-tunneling.

Not only the temperature dependence (as expressed in terms of activation energy), but also the bias dependence is indicative for the mechanisms behind the observed reverse junction current. The ideal current has no bias dependence (for reverse biases in excess of a few times the thermal voltage). Shockley-Read-Hall and trap-assisted tunneling have much more significant bias dependence. For Shockley-Read-Hall, the bias dependence goes approximately as the square root of the voltage. For trap-assisted tunneling, due to the field-enhancement, the bias dependence is larger. The largest bias dependence however is seen in case of band-to-band tunneling.

In conclusion, inspection of both temperature and bias dependence of the reverse current helps to identify the relevant leakage mechanism(s) in the junction component under investigation.

Extraction Shockley-Read-Hall and trap-assisted tunneling parameters

The fitting of Shockley-Read-Hall and trap-assisted tunneling parameters goes as follows. First, one needs to initialize the relevant parameters:

1. **MEFFTATBOT** should be initialized to 0.25. It will be fitted to the data later and affects the bias dependence of the trap-assisted tunneling current.

2. **XJUNSTI** or **XJUNGAT** should be initialized to a physically reasonable value (between 10 and 100 nm for modern CMOS). There is obviously no **XJUN** for the bottom component.

3. **CTATBOT** = **CSRHBOT**. A good starting value is found as follows. First, set **CTATBOT** and **CSRHBOT** equal to 1 and calculate the junction current. The required starting value is now found by averaging the ratio of measured and modelled currents for those reverse-bias points which are selected using the activation-energy method. A suitable criterion to select those bias points is $0.3\ \mathrm{V} < \mathrm{E}_{\mathrm{act}} < 0.7\ \mathrm{V}$.

After this initialization the parameters $\mathbf{CTATBOT} = \mathbf{CSRHBOT}$, $\mathbf{MEFFTATBOT}$ are optimized by a least-square fit of the parameters to the measured data. For the STI-edge and gate-edge components also the parameters $\mathbf{XJUNSTI}$ resp. $\mathbf{XJUNGAT}$ may be optimized. Usually a good fit can be achieved while retaining the identity $\mathbf{CTATBOT} = \mathbf{CSRHBOT}$. The parameter $\mathbf{MEFFTATBOT}$ is sometimes seen to deviate from the value of 0.25 expected theoretically. One should be able to retain a physically reasonable value for the $\mathbf{XJUN}$ parameter, in case of STI-edge and gate-edge components, although it is difficult to retain the expected identity $\mathbf{XJUNSTI} = \mathbf{XJUNGAT}$.

Extraction band-to-band tunneling parameters

If band-to-band tunneling is of importance, one needs to initialize the relevant parameters:

1. $\mathbf{FBBTRBOT}$ should be initialized to 1×10^9 V/m. It will be fitted to the data later, and affects the bias dependence of the band-to-band tunneling current.

2. $\mathbf{STFBBTBOT}$ should be initialized to -1×10^{-3}. It will be fitted to the data later, and affects the temperature dependence dependence of the band-to-band tunneling current.

3. $\mathbf{CBBTBOT}$. A good starting value is found as follows. First, set $\mathbf{CBBTBOT}$ to 1 and calculate the junction current. The required starting value is now found by averaging the ratio of measured and modelled currents for those reverse-bias points which are selected using the activation-energy method. A suitable criterion to select those bias points is $E_{\rm act} < 0.2$ V.

After this initialization the parameters are optimized by a least-square fit of the parameters to the measured data.

Extraction avalanche breakdown parameters

The breakdown voltage $\mathbf{VBRBOT}$ is easily found by inspection of the breakdown measurement curves: at $V = -\mathbf{VBRBOT}$ a sharp increase in the current is observed. The parameter $\mathbf{PBRBOT}$ can be used to tune the onset to breakdown. Again, a least-squares curve fit can be used to get a good fit. It is important to check that the Shockley-Read-Hall, trap-assisted-tunneling, and band-to-band tunneling model extrapolate well to the regime of avalanche breakdown. Sometimes, one needs to tune the corresponding parameters slightly to accomplish this.

6.6 General extraction scheme

Here we list a general extraction scheme which should work for most junctions. But please be aware that parameter extraction can never be a “push-button” exercise. The parameter extraction may have to be adapted to specific cases.

1. fit CV parameters;

2. fit ideal current parameters;

3. fit Shockley-Read-Hall and trap-assisted tunneling parameters;

4. fit band-to-band tunneling parameters;

5. fit full IV curves, except avalanche curve, once more with all relevant parameters;

6. fit avalanche breakdown parameters;

7. re-fit CV parameters (because bandgap voltage may have changed);

8. re-fit full IV curves, except avalanche curve, once more with all relevant parameters, except the bandgap voltage: this is needed because the capacitance may have changed, which affects the current;

9. calculate all model curves once more.

6.7 Simulation time considerations

MOSFET junction models are computationally expensive by their very nature: every MOSFET has at least *two* junctions (source, drain); each junction has *three* components (bottom, STI-edge, gate-edge); each current component, in turn, can have as much as *five* different conduction mechanisms (ideal, SRH, TAT, BBT, avalanche). Moreover, the physics of junctions is ruled by computationally expensive functions such as powers and exponents.

JUNCAP2 has been constructed in such a way that calculations are skipped when junction components and/or current mechanisms are set to zero. For instance, when BBT is not needed in the bottom component of a junction, one can set **CBBTBOT** to zero, and the corresponding calculation is entirely skipped.

Considerable amount of simulation time can be saved when negligible current contributions are completely switched off in a parameter set that is being extracted. Thus, in the above-mentioned example, instead of leaving **CBBTBOT** at a small, negligible non-zero value, one should set **CBBTBOT** to exactly zero in order to avoid unnecessary function evaluations when the model is used by circuit designers.

For a typical case, the JUNCAP2 features that are needed are given in Table 6.1. Typically, the number of current components needed is only half of the totally available current components.

JUNCAP2 feature	geometrical component		
	gate-edge	STI-edge	bottom
capacitance	•	•	•
ideal current	•		•
SRH current	•		•
TAT current	•		•
BBT current	•		
breakdown current	•		

Table 6.1: Guideline for which JUNCAP2 features to take into account in JUNCAP2 parameter extraction.

JUNCAP2 feature	parameter value needed to switch off feature		
	gate-edge	STI-edge	bottom
ideal current	$\mathbf{IDSATRBOT} = 0$	$\mathbf{IDSATRSTI} = 0$	$\mathbf{IDSATRGAT} = 0$
SRH current	$\mathbf{CSRHBOT} = 0$	$\mathbf{CSRHSTI} = 0$	$\mathbf{CSRHGAT} = 0$
TAT current	$\mathbf{CTATBOT} = 0$	$\mathbf{CTATSTI} = 0$	$\mathbf{CTATGAT} = 0$
BBT current	$\mathbf{CBBTBOT} = 0$	$\mathbf{CBBTSTI} = 0$	$\mathbf{CBBTGAT} = 0$
breakdown current	$\mathbf{VBRBOT} > 1000$	$\mathbf{VBRSTI} > 1000$	$\mathbf{VBRGAT} > 1000$

Table 6.2: How to switch off JUNCAP2 features.

For completeness, we recapitulate here once more how to switch off the different current components (see also Table 6.2): for the bottom component, the ideal current, SRH current, TAT current, and BBT current are switched off by setting the parameters $\mathbf{IDSATRBOT}$, $\mathbf{CSRHBOT}$, $\mathbf{CTATBOT}$, $\mathbf{CBBTBOT}$ to zero, respectively. The breakdown model is skipped by setting $\mathbf{VBRBOT}$ to a value larger than 1000. The procedure for STI-edge and gate-edge currents is, *mutatis mutandis*, the same. Note that it is *not* possible to switch off junction capacitances, because in JUNCAP2 the junction capacitances are internally used to calculate electric fields, and thus influence the junction currents.

Finally, when a geometrical component is not needed, the corresponding instance parameter ($\mathbf{AB}$, $\mathbf{LS}$, or $\mathbf{LG}$) can be set to zero and the calculation for that component is completely skipped. An example is the well diode of a p-channel MOSFET which has no gate-edge contribution ($\mathbf{LG} = 0$).

References

[1] JUNCAP: http://www.semiconductors.philips.com/Philips_Models/

[2] G.A.M. Hurkx, D.B.M. Klaassen, and M.P.G. Knuvers, *A new recombination model for device simulation including tunneling*, IEEE Trans. El. Dev., Vol. 39, No. 2, pp. 331–338, February 1992.

[3] W. Jin, C.H. Chan, S.K.H. Fung, and P.K. Ko, *Shot-noise-induced excess low-frequency noise in floating-body partially depleted SOI MOSFET's*, IEEE Trans. El. Dev., Vol. 46, No. 6, pp. 1180–1185, June 1999.

[4] MOS Model 9: http://www.semiconductors.philips.com/Philips_Models/

[5] http://www-device.eecs.berkeley.edu/˜bsim3/

[6] G.D.J. Smit, R. van Langevelde, A.J. Scholten, D.B.M. Klaassen, G. Gildenblat, X. Li, H. Wang, and W. Wu, *PSP 101.0*, Philips Research Technical Note TN-2006-00192, available on http://www.semiconductors.philips.com/Philips_Models/.